A Non-Stationary Mobile-to-Mobile Channel Model Allowing for Velocity and Trajectory Variations of the Mobile Stations

Wiem Dahech, Matthias Pätzold, Carlos A. Gutiérrez, and Néji Youssef

***Abstract*—In mobile-to-mobile (M2M) communication systems, both the transmitter and the receiver are moving with a certain velocity which is usually assumed to be constant over time. However, in realistic propagation scenarios, the velocity of the mobile stations (MSs) is subject to changes resulting in a non-stationary fading process. In this paper, we develop a non-stationary narrowband M2M multipath fading channel model, where the transmitter and the receiver experience changes in their velocities and trajectories. For this model, we derive expressions for the local autocorrelation function (ACF), the Wigner-Ville spectrum, the local average Doppler shift, and the local Doppler spread under isotropic scattering conditions. In addition, we investigate the correlation properties of the proposed model assuming non-isotropic scattering around the MSs. By relaxing the standard assumption of constant velocities of the MSs, our study shows that the local ACF and the Wigner-Ville spectrum differ completely from known expressions derived for wide-sense stationary (WSS) M2M channel models. Furthermore, it is shown that our model provides consistent results with respect to the Doppler spread. The proposed channel model is useful for the performance analysis of M2M communication systems under non-stationary conditions caused by velocity variations of the MSs.**

***Index Terms*—Non-isotropic scattering, local autocorrelation function, mobile-to-mobile channels, non-stationary processes, time-frequency analysis, velocity variations, Wigner-Ville spectrum.**

I. Introduction

The study of wireless mobile-to-mobile (M2M) communications has received considerable attention [2]. The reason is that this type of communication enables the development of new applications, especially for vehicle-to-vehicle systems [3] and cooperative networks [4], where a direct communication link between mobile stations (MSs) holds often without the intervention of fixed and highly elevated base stations. For the development, analysis, and optimization of M2M communication systems, adequate channel models are required.

A recurrent assumption in channel modelling is to characterize the velocity of the MSs as constant quantities seeking to obtain a channel model that fulfills the wide-sense stationary (WSS) condition over short observation intervals. Studies of a variety of WSS channel models and their statistical properties can be found in [5], [6], and the references therein. However, under real-world propagation conditions, the mobile radio channel is in general non-stationary [7], [8]. In fact, non-stationarity can be a result of moving scatterers as described in [9] and [10], where the transmitter and the receiver are assumed to be fixed but the scatterers are allowed to move. Furthermore, velocity changes of the MS could cause the channel statistics to be non-stationary. Yet, only a few studies uncover the effect of velocity variations of MSs. Dealing with this issue, a mobile communication scenario in which the transmitter is stationary while the receiver is moving with varying speed but constant angle of motion, which corresponds to a linear trajectory, has been considered in [11]. To account for the effect of changes in both speed and angle of motion of the MS, a fix-to-mobile (F2M) multipath fading channel model incorporating the effect of velocity variations has been presented in [12].

In this paper, we extend the work of [12] by modelling non-stationary M2M fading channels, where both the transmitter and the receiver may experience changes in their velocities over time. For that purpose, a two-dimensional (2D) reference model for narrowband single-input single-output (SISO) M2M channels has been derived based on the geometrical two-ring scattering model. Time-frequency analysis techniques are utilized as a mathematical framework for studying the statistical behavior of the proposed non-stationary M2M channel model. A review of time-frequency analysis techniques can be found in [13], [14], and [15]. In this contribution, we deal with the Wigner-Ville distribution, which is one of the most common quadratic time-frequency representations, as it satisfies many desirable properties, including the marginal and total energy properties [13]. By utilizing time-frequency analysis techniques, we provide a closed-form expression for the local autocorrelation function (ACF), from which we derive the corresponding local power spectral density (PSD), the local average Doppler shift, and the local Doppler spread. It is shown that variations in the speed and the angle of motion of the MSs have a significant impact on the statistics of the channel. Thus, the proposed channel model will be useful for the characterization and analysis of M2M communication systems operating in non-stationary propagation conditions. Although, the focus of this work is on the analysis of SISO channels, the extension to non-stationary multiple-input multiple-output (MIMO) channels is straightforward, since the temporal local ACF is the same for all sub-channels and the spatial cross-

Manuscript received March 23, 2016; revised June 22, 2016 and October 11, 2016; accepted January 10, 2017.

W. Dahech and N. Youssef are with the Université de Carthage, Ecole Supérieure des Communications de Tunis, 2083 EL Ghazala, Ariana, Tunisia.

M. Pätzold is with the Faculty of Engineering and Science, University of Agder, NO-4898 Grimstad, Norway.

C. A. Gutiérrez is with the Faculty of Science, Universidad Autonoma de San Luis Potosi, San Luis Potosi 78290, Mexico.

Part of this work has been presented at the $9th$ European Conference on Antennas and Propagation (EuCAP'15), Lisbon, Portugal, April 2015 [1].

correlation function is not influenced by the assumed scattering conditions [16].

Another insight of this paper is related to the physical inconsistency problem with respect to the Doppler spread encountered in [12], where it has been observed that the Doppler spread derived from the local ACF exceeds physically reasonable values if the MS changes its velocity. This inconsistency problem arises in non-stationary channels if an inappropriate relationship is used between the instantaneous channel phase and the instantaneous angular frequency. It is shown that the Doppler spread-inconsistency problem can be solved by defining the angular frequency as the rate of change of the argument of the complex channel gain. For stationary processes, where the transmitter and the receiver are moving with constant velocities, the angular frequency of each propagation path is constant and proportional to the corresponding time invariant Doppler shift. However, if the MSs are moving with varying velocities, then the angular frequency is time dependent and referred to as the instantaneous angular frequency. The concept of instantaneous angular frequency [17] is of significant practical importance for non-stationary signals. Nevertheless, the application of the concept of angular frequency to non-stationary mobile radio channels has not been evident and was the source of misunderstandings and confusions. For instance, when dealing with non-stationary mobile radio channels, the correct relation between the instantaneous frequency and the total phase changes has not been taken into account in many studies, e.g., [1], [11], [12], [18], [19], where the constant Doppler shifts have simply been substituted by time-varying Doppler shifts. However, this procedure leads to a physical inconsistency with respect to the Doppler spread [12]. In this paper, we resolve the inconsistency problem by taking profit of the concept of instantaneous frequency. From this perspective alone, the paper contributes to a better physical understanding of M2M channels subject to velocity variations.

Aside from the non-stationarity aspect, realistic M2M fading channels exhibit in general non-isotropic scattering which results in an asymmetric Doppler PSD. While the modelling of stationary M2M channels under non-isotropic scattering conditions has extensively been studied in the literature [20]–[22], there are only few studies devoted to the statistical characterization of M2M channels taking into account the joint effect of non-stationarity and non-isotropic scattering. For instance, the authors of [23] have investigated the statistical properties of a non-stationary M2M channel model with time dependent angles of departure (AODs) and angles of arrival (AOAs) under non-isotropic scattering conditions based on the geometrical T-junction model. In [24], a non-stationary non-isotropic F2M channel model has been analysed under the assumption that the MS follows a semi-random movement which has been modelled by a Brownian motion process with drift. It is worth mentioning that the study reported in [25] has demonstrated that the non-stationarity assumption contradicts the commonly made assumption of isotropic scattering. Therefore, the modelling of more realistic M2M channels calls for a combination of non-stationarity aspects and non-isotropic scattering effects. In this regard, we investigate the correlation properties of the proposed non-stationary M2M channel model

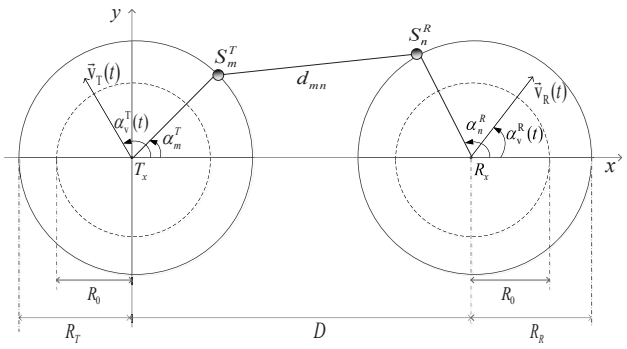

Fig. 1: The geometrical two-ring model, at the starting time t_0, wherein the transmitter T_x and the receiver R_x might change their velocities.

under non-isotropic scattering conditions, where the versatile von Mises distribution [26] is considered for modelling the AODs and AOAs. We provide a closed-form expression for the local ACF that reveals both the effect of velocity variations of the MSs and the impact of non-isotropic scattering. The obtained expression includes both the local ACF derived under the assumption of isotropic scattering and the ACF of WSS double Rayleigh M2M channels as special cases.

The rest of this paper is organized as follows. In Section II, we derive the non-stationary M2M channel model starting from an extended version of the geometrical two-ring scattering model. In Section III, we study the effect of velocity variations of the MSs on the statistical properties of the proposed channel model under isotropic scattering conditions. The extension of the analysis to non-isotropic scattering is the topic of Section IV. Numerical results for specific propagation scenarios are presented in Section V. Finally, the conclusions are drawn in Section VI.

II. The Non-Stationary M2M Channel Model

We consider a narrowband M2M multipath fading channel model, where the transmitter and the receiver are moving with varying velocities. Both terminals are equipped with omnidirectional antennas. They are supposed to be surrounded by a large number of scatterers located on two rings centred on the MSs. We start our analysis by describing first the geometrical two-ring scattering model that serves as a starting point for the derivation of the reference channel model.

A. The Geometrical Two-Ring Scattering Model

We consider a geometrical two-ring scattering model as illustrated in Fig. 1. This model includes a mobile transmitter T_x and a mobile receiver R_x with two statistically independent groups of effective scatterers S_m^T $(m = 1, 2, ..., M)$ and S_n^R $(n = 1, 2, ..., N)$ around each terminal, where M and N denote the number of scatterers around the transmitter T_x and the receiver R_x, respectively. The two-ring scattering model is based on the assumption that the local scatterers are randomly placed on two separate rings with radii R_T and R_R. The rings

of the scatterers are also assumed to be centred on the positions of the transmitter T_x and the receiver R_x. Under narrowband conditions, these assumptions could be fulfilled by using rings of effective scatterers instead of real local scatterers around T_x and R_x. Therefore, the radii R_T and R_R are supposed to be identical for each reflection caused by the effective scatterers S_m^T and S_n^R, respectively. The two rings of the scatterers are assumed to be fixed over the observation period T_0 and separated by a relatively large distance D compared to the radii R_T and R_R, i.e., $\max\{R_T, R_R\} \ll D$. In addition, we assume that the transmitter T_x and the receiver R_x are moving during the observation period T_0 with varying velocities inside the inner rings of radius R_0 such that $\min\{R_T, R_R\} \gg R_0$. Under this assumption, the inner rings of radii R_0 restrict the mobility range of the transmitter and the receiver, such that the AODs α_m^T and the AOAs α_n^R are time invariant and can be considered as independent random variables. The hypothetical inner rings of radii R_0 have been introduced to limit the mobility range of the MSs during the observation period. Furthermore, by taking into account that the rings of scatterers are assumed to be fixed, the distance D between their corresponding centres does not change over the time, i.e., D is constant for $t \in [0, T_0]$. In addition, we consider a double interaction between the scatterers around the transmitter and the receiver under non-line-of-sight (NLOS) conditions. That is, the plane waves emitted from the transmitter T_x are first captured by the scatterers S_m^T and then reach the scatterers S_n^R before arriving at the receiver R_x. According to the studies in [27], [28], the double interaction with interfering objects is prevalent in highway and urban environments, where the MSs are assumed to be surrounded by a large number of fixed scatterers. Even though in reality the scatterers are not arranged around the Tx and the Rx in regular-shaped geometries, the two-ring scattering model provides an abstraction of the propagation environment that has been shown to be suitable for the modelling of non-stationary M2M radio channels [7]. The novelty of the proposed model in comparison to the stationary M2M channel model arises from the incorporation of the effect of velocity variations of the MSs. Indeed, the transmitter T_x and the receiver R_x are moving with varying velocities determined by the speeds $\mathrm{v}_T(t)$, $\mathrm{v}_R(t)$ and the angles of motion $\alpha_{\mathrm{v}}^T(t)$, $\alpha_{\mathrm{v}}^R(t)$, respectively. As a consequence of the velocity variations of the MSs, the resulting Doppler shifts are time dependent, as described in the next subsection.

B. Analysis of the Doppler Effect

Recall that the velocity is defined as a vector that represents the rate of change of the position of the MS with respect to time. With the speed $\mathrm{v}_i(t)$ and the angle of motion $\alpha_{\mathrm{v}}^i(t)$, we can present the velocity $\vec{\mathrm{v}}_i(t)$ of the transmitter ($i = T$) and the receiver ($i = R$) in vector form as $\vec{\mathrm{v}}_i(t) = \mathrm{v}_i(t)\exp\{j\alpha_{\mathrm{v}}^i(t)\}$. If there is any change in speed and/or direction, then the MS changes its velocity. The Taylor series expansions of the time variant speed $\mathrm{v}_i(t)$ and angle of motion $\alpha_{\mathrm{v}}^i(t)$ can be represented at $t = t_0$ as

$$\mathrm{v}_i(t) = \mathrm{v}_i(t_0) + \frac{d\mathrm{v}_i(t)}{dt}\Big|_{t_0}(t-t_0) + \frac{1}{2}\frac{d^2\mathrm{v}_i(t)}{dt^2}\Big|_{t_0}(t-t_0)^2 + \cdots \quad (1)$$

$$\alpha_{\mathrm{v}}^i(t) = \alpha_{\mathrm{v}}^i(t_0) + \frac{d\alpha_{\mathrm{v}}^i(t)}{dt}\Big|_{t_0}(t-t_0) + \frac{1}{2}\frac{\alpha_{\mathrm{v}}^i(t)}{dt^2}\Big|_{t_0}(t-t_0)^2 + \cdots . \quad (2)$$

By setting $t_0 = 0$ and using the first two terms of the Taylor series in (1) and (2), $\mathrm{v}_i(t)$ and $\alpha_{\mathrm{v}}^i(t)$ can be expressed as

$$\mathrm{v}_i(t) = \mathrm{v}_0^i + a_0^i t \quad (3)$$

$$\alpha_{\mathrm{v}}^i(t) = \alpha_0^i + b_0^i t \quad (4)$$

where $\mathrm{v}_0^i = \mathrm{v}_i(0)$ and $\alpha_0^i = \alpha_{\mathrm{v}}^i(0)$ are constants denoting, respectively, the initial speed and the initial angle of motion at time $t_0 = 0$. The symbols $a_0^i = d\mathrm{v}_i(t)/dt|_{t_0=0}$ and $b_0^i = d\alpha_{\mathrm{v}}^i(t)/dt|_{t_0=0}$ denote constants representing the speed acceleration and the angular speed, respectively. A novel feature of our work is that each MS can change its speed and direction over time by introducing the speed acceleration a_0^i and the angular speed b_0^i parameters, respectively. It is important to mention that the velocity model described by (3) and (4) is not generally valid and may not adequately capture specific mobility characteristics. Nevertheless, this model is useful to describe the velocity changes in micro-scale mobility scenarios limited by circles of relatively small radii $R_0 \ll R_T, R_R$. Accordingly, the corresponding non-stationary M2M channel model with interactions between interfering objects is recommended for the modelling of some special vehicular communication scenarios, where the vehicles are surrounded by a large number of local scatterers. In such propagation scenarios, the vehicles can move with time variant velocities under the assumption of NLOS propagation conditions, which are typical for dense urban areas. Furthermore, the time variant velocity vector $\vec{\mathrm{v}}_i(t)$ includes several trajectories as special cases. For instance, the MS follows a straight line trajectory with a uniform acceleration (deceleration) if $b_0^i = 0$ and $a_0^i > 0$ ($a_0^i < 0$). On the other hand, if $a_0^i = 0$ and $b_0^i \neq 0$, then the MS is in uniform circular motion. Finally, the trajectory of the transmitter T_x or the receiver R_x follows a spiral course if the speed $\mathrm{v}_i(t)$ and angle of motion $\alpha_{\mathrm{v}}^i(t)$ are time variant, i.e., $a_0^i \neq 0$ and $b_0^i \neq 0$. In this case, the maximum Doppler frequency $f_{\max}^i(t)$ is a time dependent function, which can be expressed in terms of the carrier frequency f_0 and the speed of light c_0 as $f_{\max}^i(t) = f_0\mathrm{v}_i(t)/c_0$. This equation can also be written by using (3) as

$$f_{\max}^i(t) = f_{\max_0}^i + \dot{f}_{\max}^i t \quad (5)$$

where $f_{\max_0}^i = f_0\mathrm{v}_0^i/c_0$ and $\dot{f}_{\max}^i = f_0 a_0^i/c_0$.

The total Doppler shifts $f_{mn}(t)$ can be presented as a sum of the Doppler shifts $f_m^T(t)$ and $f_n^R(t)$ caused by the motion of the transmitter and the receiver, respectively, i.e.,

$$f_{mn}(t) = f_m^T(t) + f_n^R(t) \quad (6)$$

for $m = 1, 2, ..., M$ and $n = 1, 2, ..., N$, where

$$f_m^T(t) = f_{\max}^T(t)\cos\left(\alpha_m^T - \alpha_{\mathrm{v}}^T(t)\right) \quad (7)$$

and

$$f_n^R(t) = f_{\max}^R(t)\cos\left(\alpha_n^R - \alpha_{\mathrm{v}}^R(t)\right). \quad (8)$$

As a consequence of the time variant velocities of the MSs and of the random behavior of α_m^T and α_n^R, it follows that the

total Doppler shifts $f_{mn}(t)$ are stochastic processes. This is in contrast to the conventional case in which the Doppler shifts are treated as random variables. In the next subsection, we investigate the statistical properties of the time variant Doppler shifts.

C. Statistical Properties of the Doppler Shifts

Under isotropic scattering conditions, it can be shown that the probability density functions (PDFs) of the time variant Doppler shifts $f_m^T(t)$ and $f_n^R(t)$ can be expressed as

$$p_{f_m^T}(f;t) = \begin{cases} \frac{1}{\pi f_{\max}^T(t)\sqrt{1-\left(f/f_{\max}^T(t)\right)^2}}, & |f| \le f_{\max}^T(t) \\ 0, & |f| > f_{\max}^T(t) \end{cases} \tag{9}$$

$$p_{f_n^R}(f;t) = \begin{cases} \frac{1}{\pi f_{\max}^R(t)\sqrt{1-\left(f/f_{\max}^R(t)\right)^2}}, & |f| \le f_{\max}^R(t) \\ 0, & |f| > f_{\max}^R(t) \end{cases} \tag{10}$$

respectively. For the special case in which an MS moves with constant speed $\mathrm{v}^i(t) = \mathrm{v}_0^i$, where $i \in \{T, R\}$, we obtain $f_{\max}^i(t) = f_{\max_0}^i = f_0 \mathrm{v}_0^i / c_0$. Thus, the PDF of each Doppler shift is equal to the Clarke distribution [29]. By assuming double interactions between the transmitter and the receiver scatterers under isotropic scattering conditions, the AOD α_m^T and the AOA α_n^R are independent and identically distributed (i.i.d.) random variables characterized by a uniform distribution over 0 to 2π. As a consequence, the two partial Doppler shifts $f_m^T(t)$ and $f_n^R(t)$ are also statistically independent for any value of m and $n \neq m$. Hence, the PDF of the sum in (6), representing the distribution of the total Doppler shift $f_{mn}(t)$, can be computed as follows

$$p_{f_{mn}}(f;t) = \left(p_{f_m^T} * p_{f_n^R}\right)(f;t) \tag{11}$$

where the symbol $*$ denotes the convolution operator. Substituting (9) and (10) in (11), and using [30, Eq. (3.147-5)], allows us to write the time dependent PDF of $f_{mn}(t)$ as

$$p_{f_{mn}}(f;t) = \frac{K\left(\sqrt{\frac{\left(f_{\max}^T(t)+f_{\max}^R(t)\right)^2 - f^2}{4 f_{\max}^T(t) f_{\max}^R(t)}}\right)}{\pi^2 \sqrt{f_{\max}^T(t)\, f_{\max}^R(t)}} \tag{12}$$

where $K(\cdot)$ represents the complete elliptic integral of the first kind [30, Eq. (8.110-3)].

Two important statistical quantities characterizing the time-varying PDF $p_{f_{mn}}(f;t)$ are the time variant average Doppler shift and the time variant Doppler spread. The time variant average Doppler shift is defined as the first moment of $p_{f_{mn}}(f;t)$, whereas the time variant Doppler spread is obtained as the square root of the second central moment of $p_{f_{mn}}(f;t)$. A common approach to investigate the above two quantities is the use of the characteristic function $\psi_{f_{mn}}(\tau;t)$ of $f_{mn}(t)$. Applying [30, Eq. (6.611-1)], we can write the time dependent characteristic function $\psi_{f_{mn}}(\tau;t)$ as

$$\psi_{f_{mn}}(\tau;t) = J_0\left(2\pi f_{\max}^T(t)\,\tau\right) J_0\left(2\pi f_{\max}^R(t)\,\tau\right) \tag{13}$$

where $J_0(\cdot)$ denotes the zeroth-order Bessel function of the first kind [30, Eq. (8.402)]. The characteristic function $\psi_{f_{mn}}(\tau;t)$ presented in (13) equals the product of two Bessel functions which are dependent on the time varying Doppler frequencies $f_{\max}^T(t)$ and $f_{\max}^R(t)$. Invoking the moment theorem [31, Eq. (4.9)] allows us to compute the time variant average Doppler shift $B_{f_{mn}}^{(1)}(t)$ of the non-stationary channel model as

$$B_{f_{mn}}^{(1)}(t) := \frac{1}{2\pi j}\dot{\psi}_{f_{mn}}(0;t) \tag{14}$$

where $\dot{\psi}_{f_{mn}}(\tau;t) = d\psi_{f_{mn}}(\tau;t)/d\tau$. Substituting (13) in (14) gives

$$B_{f_{mn}}^{(1)}(t) = 0. \tag{15}$$

Similarly, the time variant Doppler spread $B_{f_{mn}}^{(2)}(t)$, defined as the square root of the second moment of $p_{f_{mn}}(f;t)$, can be expressed by means of the characteristic function $\psi_{f_{mn}}(\tau,t)$ as

$$B_{f_{mn}}^{(2)}(t) := \frac{1}{2\pi}\sqrt{-\ddot{\psi}_{f_{mn}}(0,t)}. \tag{16}$$

Thus, substituting (13) in (16) leads to

$$B_{f_{mn}}^{(2)}(t) = \sqrt{\frac{\left(f_{\max}^T(t)\right)^2 + \left(f_{\max}^R(t)\right)^2}{2}}. \tag{17}$$

We notice that the Doppler spread of the stationary M2M model is included in the time variant Doppler spread presented in (17) as a special case if the speed accelerations a_0^T and a_0^R are equal to zero. In this case, we obtain $B_{f_{mn}}^{(2)}(t) = B_{f_{mn}}^{(2)} = \sqrt{\left(f_{\max_0}^T\right)^2 + \left(f_{\max_0}^R\right)^2}/\sqrt{2}$. Furthermore, it should be noticed that, under isotropic scattering conditions, the distribution of the Doppler shifts in (12) depends on the maximum Doppler frequencies $f_{\max}^T(t)$ and $f_{\max}^R(t)$ caused by the motion of the transmitter and the receiver, respectively, but not on the corresponding angles of motion $\alpha_{\mathrm{v}}^T(t)$ and $\alpha_{\mathrm{v}}^R(t)$. This explains why the characteristic quantities $B_{f_{mn}}^{(1)}(t)$ and $B_{f_{mn}}^{(2)}(t)$ of the non-stationary model are independent of the angles of motion $\alpha_{\mathrm{v}}^T(t)$ and $\alpha_{\mathrm{v}}^R(t)$. Based on the above analysis, we present the reference model in the next subsection.

D. The Reference Model

Starting from the proposed geometrical model, we derive an analytical model which will be referred to as the reference model. This model is described by an ideal non-wide-sense stationary (NWSS) complex Gaussian process and aims to reproduce the channel characteristics observed in real-world propagation scenarios. The derivation of the reference model is of central importance, as it provides a theoretical framework for the performance analysis of mobile communication systems. Furthermore, based on the theoretical reference model, a realizable simulation model can be derived by applying the principle of deterministic channel modelling [6, pp. 101]. In mobile radio communications, the validation of the reference model and the corresponding simulation model should be performed by means of real-world measurement results. In what follows, we derive the reference model for the proposed non-stationary M2M channel. Independently of the position of the transmitter T_x and the receiver R_x, we assume double interactions between interfering objects caused by circularly distributed local scatterers on fixed rings centred on T_x and

R_x. Under this assumption, the complex channel gain $\mu(t) = \mu_I(t) + j\mu_Q(t)$, describing the M2M channel model in the complex baseband, can be derived from the geometrical two-ring model shown in Fig. 1 to yield

$$\mu(t) = \lim_{\substack{M\to\infty \\ N\to\infty}} \sum_{m=1}^{M}\sum_{n=1}^{N} c_{mn} e^{j\{\nu_{mn}(t)+\theta_{mn}-k_0 D_{mn}\}} \tag{18}$$

where $k_0 = 2\pi/\lambda_0$ is the free-space wave number and λ_0 denotes the wavelength. In (18), c_{mn} and θ_{mn} stand for the joint gain and the joint phase shift, respectively. The joint phase shift θ_{mn} can be expressed as $\theta_{mn} = \theta_m + \theta_n (\mathrm{mod}\ 2\pi)$, where θ_m and θ_n are supposed to be i.i.d. random variables, each of which is uniformly distributed over the interval $[0, 2\pi)$. The phase shifts θ_m and θ_n are caused by the interaction of the transmitted plane waves with the scatterers S_m^T and S_n^R, respectively. The path gains c_{mn} are also taken as i.i.d. random variables characterized by $E\left\{c_{mn}^2\right\} = 2\sigma_0^2/(MN)$, where $E\{\cdot\}$ stands for the expectation operator, and $2\sigma_0^2$ is the mean power of the complex channel gain $\mu(t)$. The phase change $k_0 D_{mn}$ in (18) is determined by the total distance D_{mn} that a plane wave travels from T_x to R_x via the scatterers S_m^T and S_n^R. By invoking the assumption $R_0 \ll R_T, R_R$, the distances covered by the MSs during the observation period T_0 are relatively limited compared to the radii R_T and R_R. Therefore, the distances between the MSs and the scatterers can be approximated by the radii R_T and R_R. In this case, the phase component $k_0 D_{mn}$ can be written as

$$k_0 D_{mn} \approx \frac{2\pi}{\lambda_0}\left(R_T + d_{mn} + R_R\right) \tag{19}$$

where d_{mn} is the distance between the scatterers S_m^T and S_n^R (see Fig. 1). Since the rings of the scatterers are assumed to be fixed, the distance d_{mn} is time independent. Recall that we have assumed that the transmitter T_x and the receiver R_x are allowed to move inside circles of radii R_0 with $R_T, R_R \gg R_0$, such that the lengths of the trajectories along which the MSs are travelling are small compared to the radii R_T and R_R. Thus, the distance d_{mn} can be written as

$$\begin{aligned} d_{mn} \approx \Bigg(&\left(D + R_R\cos\left(\alpha_n^R\right) - R_T\cos\left(\alpha_m^T\right)\right)^2 \\ &+\left(R_R\sin\left(\alpha_n^R\right) - R_T\sin\left(\alpha_m^T\right)\right)^2\Bigg)^{\frac{1}{2}}. \end{aligned} \tag{20}$$

Since the ring radii R_T and R_R are much smaller than the distance D, i.e., $R_T, R_R \ll D$, we can profit from the approximation $\sqrt{1+x} \approx 1 + x/2$ $(x \ll 1)$ to express the distance d_{mn} as

$$d_{mn} \approx D - R_T\cos\left(\alpha_m^T\right) + R_R\cos\left(\alpha_n^R\right). \tag{21}$$

Furthermore, the phase changes $\nu_{mn}(t)$ in (18) are due to the motion of the transmitter T_x and the receiver R_x. For the proposed model, the channel is NWSS due to the velocity variations of the MSs which affect the phase changes $\nu_{mn}(t)$. In order to determine the expression of $\nu_{mn}(t)$, we apply the concept of the instantaneous frequency which was originally shown to be useful for the estimation and modelling of time varying signals [17]. The instantaneous frequency given by the Doppler shift $f_{mn}(t)$ can be expressed as [17]

$$f_{mn}(t) = \frac{1}{2\pi}\frac{d\phi_{mn}(t)}{dt} \tag{22}$$

where $\phi_{mn}(t)$ represents the total phase change of the complex channel gain $\mu(t)$, i.e., $\phi_{mn}(t) = \nu_{mn}(t) + \theta_{mn} - k_0 D_{mn}$. According to (22), $\phi_{mn}(t)$ can be expressed as

$$\phi_{mn}(t) = 2\pi\int_{-\infty}^{t} f_{mn}(x)dx = \underbrace{2\pi\int_{-\infty}^{0} f_{mn}(x)dx}_{\phi_{mn}(0)} + 2\pi\int_{0}^{t} f_{mn}(x)dx. \tag{23}$$

By substituting the expression of the total Doppler shifts $f_{mn}(t)$ given by (6) in (23), the expression of the total phase change $\phi_{mn}(t)$ is obtained as

$$\begin{aligned} \phi_{mn}(t) = \phi_{mn}(0) &+2\pi\Bigg(\frac{\dot{f}_{\max}^T}{(b_0^T)^2}\cos\left(\alpha_m^T - \alpha_{\mathrm{v}}^T(t)\right) - \frac{f_{\max}^T(t)}{b_0^T}\sin\left(\alpha_m^T - \alpha_{\mathrm{v}}^T(t)\right) \\ &+\frac{\dot{f}_{\max}^R}{(b_0^R)^2}\cos\left(\alpha_n^R - \alpha_{\mathrm{v}}^R(t)\right) - \frac{f_{\max}^R(t)}{b_0^R}\sin\left(\alpha_n^R - \alpha_{\mathrm{v}}^R(t)\right)\Bigg). \end{aligned} \tag{24}$$

From (24), we can gain insight into the influence of the speed acceleration a_0^i on the total phase change $\phi_{mn}(t)$ through the parameter $\dot{f}_{\max}^i$, which is related to a_0^i by $\dot{f}_{\max}^i = f_0 a_0^i/c_0$, where $i \in \{T, R\}$. In the case $b_0^i = 0$ and $a_0^i \neq 0$ for $i \in \{T, R\}$, which holds if both the transmitter T_x and the receiver R_x are moving with varying speed in the same direction, the instantaneous phase $\phi_{mn}(t)$ is obtained from (24) by taking the limits $b_0^T \to 0$ and $b_0^R \to 0$, which results in

$$\begin{aligned} \phi_{mn}(t) = \phi_{mn}(0) &+2\pi\Bigg(\left[f_{\max_0}^T\cos\left(\alpha_m^T - \alpha_0^T\right) + f_{\max_0}^R\cos\left(\alpha_n^R - \alpha_0^R\right)\right]t \\ &+\left[\dot{f}_{\max}^T\cos\left(\alpha_m^T - \alpha_0^T\right) + \dot{f}_{\max}^R\cos\left(\alpha_n^R - \alpha_0^R\right)\right]\frac{t^2}{2}\Bigg). \end{aligned} \tag{25}$$

In case that only the transmitter T_x or the receiver R_x is allowed to change its angle of motion over the time, i.e., $b_0^i \neq 0$ and $b_0^l = 0$ with $\{i, l\} \in \{T, R\}$ and $i \neq l$, the instantaneous phase $\phi_{mn}(t)$ can be obtained by calculating the limit $b_0^l \to 0$ of (24) as

$$\begin{aligned} \phi_{mn}(t) = \phi_{mn}(0) &+2\pi\Bigg(\frac{\dot{f}_{\max}^i}{(b_0^i)^2}\cos\left(\alpha_q^i - \alpha_{\mathrm{v}}^i(t)\right) - \frac{f_{\max}^i(t)}{b_0^i}\sin\left(\alpha_q^i - \alpha_{\mathrm{v}}^i(t)\right) \\ &+f_{\max_0}^l\cos\left(\alpha_q^l - \alpha_0^l\right)t + \dot{f}_{\max}^l\cos\left(\alpha_q^l - \alpha_0^l\right)\frac{t^2}{2}\Bigg) \end{aligned} \tag{26}$$

where the subscript $q \in \{m, n\}$. Finally, in (23)–(26), the first term represents the unknown initial phase $\phi_{mn}(0)$ which can be identified as the time independent phase shifts of the complex channel gain $\mu(t)$ given by (18), i.e., $\phi_{mn}(0) = \theta_{mn} - k_0 D_{mn}$, whereas the second term, being a function of time, represents the phase change $\nu_{mn}(t)$ in (18). Thus, by substituting (19),

(21), and (24) in (18), the complex channel gain $\mu(t)$ of the non-stationary M2M channel model can be expressed as in (27) [see the equation at the top of the next page]. It should be mentioned that $\theta_0 = -\frac{2\pi}{\lambda_0}(R_T + R_R + D)$ is a constant phase shift which can be omitted without affecting the statistics of the reference model. It can also be noted from (27) that the complex channel gain $\mu(t)$ is not only influenced by the angular speed b_0^i, but also by the speed acceleration a_0^i via the parameter $\dot{f}_{\max}^i = f_0 a_0^i / c_0$, where $i \in \{T, R\}$.

III. Statistical Properties of the Reference Model Assuming Isotropic Scattering

In this section, we investigate the statistical properties of the proposed non-stationary M2M channel model under isotropic scattering conditions. In fact, we will study the effect of velocity variations on the main characteristic quantities of the complex channel gain $\mu(t)$ given by (27).

A. Mean Value and Variance

For the proposed non-stationary M2M channel model, the mean value of $\mu(t)$ equals

$$m_\mu = E\{\mu(t)\} = 0. \tag{28}$$

Using the relation $E\left\{c_{mn}^2\right\} = 2\sigma_0^2/MN$, we can compute the variance σ_μ^2 of $\mu(t)$ as follows

$$\sigma_\mu^2 = \mathrm{Var}\{\mu(t)\} = E\left\{\mu^*(t)\mu(t) - m_\mu^2\right\} = 2\sigma_0^2 \tag{29}$$

where $\mathrm{Var}\{\cdot\}$ denotes the variance operator and $(\cdot)^*$ denotes the complex conjugate operator. It is noteworthy that the mean value and the variance of the complex channel gain $\mu(t)$ are not influenced by the velocity variations of the MSs.

B. The Local ACF

The local ACF $r_{\mu\mu}(\tau, t)$ of the complex channel gain $\mu(t)$ is a function of the time difference τ and time t. In this paper, we consider the following definition of the local ACF proposed by Mark in [32]

$$r_{\mu\mu}(\tau, t) = E\left\{\mu^*\left(t - \frac{\tau}{2}\right)\mu\left(t + \frac{\tau}{2}\right)\right\}. \tag{30}$$

By taking into account the random characteristics of the gains c_{mn}, the AODs α_m^T, the AOAs α_n^R, and the phases θ_m and θ_n, the local ACF $r_{\mu\mu}(\tau, t)$ has to be determined using statistical expectations. Therefore, by substituting (27) in (30) and applying the expectation operator to the random variables c_{mn}, θ_m, θ_n, α_m^T, and α_n^R, an expression of the local ACF $r_{\mu\mu}(\tau, t)$ can be obtained. By using [30, Eq. (3.937-2)], the local ACF $r_{\mu\mu}(\tau, t)$ can be expressed as

$$\begin{aligned} r_{\mu\mu}(\tau, t) = 2\sigma_0^2 J_0\Bigg(2\pi\Bigg\{&\left(2\frac{f_{\max}^T(t)}{b_0^T}\right)^2 \sin^2\left(b_0^T\frac{\tau}{2}\right) \\ &+ \left(2\frac{\dot{f}_{\max}^T}{(b_0^T)^2}\sin\left(b_0^T\frac{\tau}{2}\right) - \frac{\dot{f}_{\max}^T}{b_0^T}\tau\cos\left(b_0^T\frac{\tau}{2}\right)\right)^2\Bigg\}^{\frac{1}{2}}\Bigg) \\ \cdot J_0\Bigg(2\pi\Bigg\{&\left(2\frac{f_{\max}^R(t)}{b_0^R}\right)^2 \sin^2\left(b_0^R\frac{\tau}{2}\right) \\ &+ \left(2\frac{\dot{f}_{\max}^R}{(b_0^R)^2}\sin\left(b_0^R\frac{\tau}{2}\right) - \frac{\dot{f}_{\max}^R}{b_0^R}\tau\cos\left(b_0^R\frac{\tau}{2}\right)\right)^2\Bigg\}^{\frac{1}{2}}\Bigg). \end{aligned} \tag{31}$$

From (31), we notice that the maximum Doppler frequency $f_{\max}^i(t)$ influences the local correlation properties. However, under the assumed isotropic scattering conditions, the local ACF $r_{\mu\mu}(\tau, t)$ is dependent on the velocity parameters v_0^i, a_0^i, and b_0^i, but independent of the initial angle of motion α_0^i. Depending on the speed acceleration a_0^i and the angular speed b_0^i, the following three special cases are of interest.

Case I: If $b_0^i \neq 0$ and $b_0^l = 0$ with $\{i, l\} \in \{T, R\}$ and $l \neq i$, i.e, only one MS is allowed to change its direction over time, then the local ACF $r_{\mu\mu}(\tau, t)$ is obtained by calculating the limit of (31) as $b_0^l \to 0$. In this case, $r_{\mu\mu}(\tau, t)$ can be expressed as

$$\begin{aligned} r_{\mu\mu}(\tau, t) = 2\sigma_0^2 J_0\left(2\pi f_{\max}^l(t)\,\tau\right) J_0\Bigg(2\pi\Bigg\{&\left(2\frac{f_{\max}^i(t)}{b_0^i}\right)^2 \sin^2\left(b_0^i\frac{\tau}{2}\right) \\ &+ \left(2\frac{\dot{f}_{\max}^i}{(b_0^i)^2}\sin\left(b_0^i\frac{\tau}{2}\right) - \frac{\dot{f}_{\max}^i}{b_0^i}\tau\cos\left(b_0^i\frac{\tau}{2}\right)\right)^2\Bigg\}^{\frac{1}{2}}\Bigg). \end{aligned} \tag{32}$$

Case II: If $b_0^T \to 0$ and $b_0^R \to 0$, then (31) tends to

$$r_{\mu\mu}(\tau, t) = 2\sigma_0^2 J_0\left(2\pi f_{\max}^T(t)\,\tau\right) J_0\left(2\pi f_{\max}^R(t)\,\tau\right). \tag{33}$$

The result in (33) shows that the normalized local ACF $r_{\mu\mu}(\tau, t)/(2\sigma_0^2)$ is equivalent to the time dependent characteristic function $\psi_{f_{mn}}(\tau; t)$ in (13) if the MSs are allowed to change only their speeds over time t.

Case III: For the special case where the process $\mu(t)$ is WSS, i.e., $a_0^i = b_0^i = 0$, the local ACF $r_{\mu\mu}(\tau, t)$ presented in (33) becomes time invariant yielding the known result $r_{\mu\mu}(\tau) = 2\sigma_0^2 J_0(2\pi f_{\max_0}^T \tau) J_0(2\pi f_{\max_0}^R \tau)$ which can be found in [33, Eq. (35)].

C. The Wigner-Ville Spectrum

The Wigner-Ville distribution is defined as [13]

$$W_{\mu\mu}(f, t) = \int_{-\infty}^{+\infty} \mu^*\left(t - \frac{\tau}{2}\right)\mu\left(t + \frac{\tau}{2}\right) e^{-j2\pi f\tau} d\tau. \tag{34}$$

By applying the expectation operator $E\{\cdot\}$ to both sides of (34) and using the local ACF $r_{\mu\mu}(\tau, t)$ in (31), we obtain the Wigner-Ville spectrum $S_{\mu\mu}(f, t)$ in the following form [34]

$$S_{\mu\mu}(f, t) = \int_{-\infty}^{+\infty} r_{\mu\mu}(\tau, t) e^{-j2\pi f\tau} d\tau. \tag{35}$$

$$\mu(t) = \lim_{\substack{M\to\infty \\ N\to\infty}} \sum_{m=1}^{M}\sum_{n=1}^{N} c_{mn} e^{j\left\{\theta_{mn} - \frac{2\pi}{\lambda_0}\left(-R_T\cos\left(\alpha_m^T\right) + R_R\cos\left(\alpha_n^R\right)\right) + \theta_0\right\}} \cdot e^{j\left\{2\pi\left(\frac{\dot{f}_{\max}^T}{\left(b_0^T\right)^2}\cos\left(\alpha_m^T - \alpha_{\mathrm{v}}^T(t)\right) - \frac{f_{\max}^T(t)}{b_0^T}\sin\left(\alpha_m^T - \alpha_{\mathrm{v}}^T(t)\right) + \frac{\dot{f}_{\max}^R}{\left(b_0^R\right)^2}\cos\left(\alpha_n^R - \alpha_{\mathrm{v}}^R(t)\right) - \frac{f_{\max}^R(t)}{b_0^R}\sin\left(\alpha_n^R - \alpha_{\mathrm{v}}^R(t)\right)\right)\right\}}. \tag{27}$$

Although the Wigner-Ville spectrum $S_{\mu\mu}(f,t)$ is the Fourier transform of the local ACF $r_{\mu\mu}(\tau,t)$, it cannot be considered as a generalization of the PSD of stationary processes. Regarding the local ACF $r_{\mu\mu}(\tau,t)$ described by (31) and (32), the integral in (35) has to be solved numerically. However, if the MSs are moving with varying speed along a fixed direction, i.e., $\alpha_{\mathrm{v}}^i(t) = \alpha_0^i$ ($b_0^i = 0$), then we obtain the following closed-form expression for the Wigner-Ville spectrum

$$S_{\mu\mu}(f,t) = \begin{cases} \dfrac{2\sigma_0^2 K\left(\sqrt{\frac{\left(f_{\max}^T(t) + f_{\max}^R(t)\right)^2 - f^2}{4 f_{\max}^T(t) f_{\max}^R(t)}}\right)}{\pi^2\sqrt{f_{\max}^T(t) f_{\max}^R(t)}}, & |f| \le f_{\max}^T(t) + f_{\max}^R(t) \\ 0, & |f| > f_{\max}^T(t) + f_{\max}^R(t). \end{cases} \tag{36}$$

Only in this case, the Doppler PSD $S_{\mu\mu}(f,t)$ is proportional to the PDF $p_{f_{mn}}(f;t)$ presented in (12), i.e., $S_{\mu\mu}(f,t) = 2\sigma_0^2 p_{f_{mn}}(f;t)$, which is in accordance with the relation $S_{\mu\mu}(f) = 2\sigma_0^2 p_{f_{mn}}(f)$ which is well known for stationary channel models.

D. Local Average Doppler Shift and Local Doppler Spread

In this subsection, we derive closed-form expressions for the local average Doppler shift $B_{\mu\mu}^{(1)}(t)$ and the local Doppler spread $B_{\mu\mu}^{(2)}(t)$ by means of the local ACF $r_{\mu\mu}(\tau,t)$ given by (31).

The local average Doppler shift $B_{\mu\mu}^{(1)}(t)$ is defined as

$$B_{\mu\mu}^{(1)}(t) := \frac{1}{2\pi j}\frac{\dot{r}_{\mu\mu}(0,t)}{r_{\mu\mu}(0,t)} \tag{37}$$

where $\dot{r}_{\mu\mu}(0,t)$ is the derivative of the local ACF $r_{\mu\mu}(\tau,t)$ with respect to τ at $\tau = 0$. For the isotropic scattering case, we obtain $B_{\mu\mu}^{(1)}(t) = 0$ after substituting (31) in (37).

The local Doppler spread $B_{\mu\mu}^{(2)}(t)$ is defined as

$$B_{\mu\mu}^{(2)}(t) := \frac{1}{2\pi}\sqrt{\left(\frac{\dot{r}_{\mu\mu}(0,t)}{r_{\mu\mu}(0,t)}\right)^2 - \frac{\ddot{r}_{\mu\mu}(0,t)}{r_{\mu\mu}(0,t)}}. \tag{38}$$

By using (31), we can present the local Doppler spread $B_{\mu\mu}^{(2)}(t)$ in closed form as

$$B_{\mu\mu}^{(2)}(t) = \sqrt{\frac{\left(f_{\max}^T(t)\right)^2 + \left(f_{\max}^R(t)\right)^2}{2}}. \tag{39}$$

Thus, (39) shows that the Doppler spread $B_{\mu\mu}^{(2)}(t)$ of the non-stationary stochastic process $\mu(t)$ is no longer constant but time dependent. Furthermore, we notice that the local Doppler spread $B_{\mu\mu}^{(2)}(t)$ presented in (39) is equal to the previous expression of the time variant Doppler spread $B_{f_{mn}}^{(2)}(t)$ presented in (17). This comparison demonstrates that the proposed non-stationary M2M channel model is consistent with respect to the Doppler spread. The same statement holds for the average Doppler shift $B_{\mu\mu}^{(1)}(t)$ and the time variant Doppler shift $B_{f_{mn}}^{(1)}(t)$. Therefore, by using the relationship between the instantaneous frequency and the instantaneous phase given in (23), we can solve the inconsistency problem of non-stationary channels with respect to the Doppler spread reported in [12]. In fact, for stationary processes, where the transmitter and the receiver are moving with constant velocities, the Doppler shift is time independent, i.e., $f_{mn}(t) = f_{mn}$, and the corresponding angular Doppler shift is given by $2\pi f_{mn} t$. The generalisation of the above relationship to non-stationary signals, by simply substituting f_{mn} by the time variant Doppler shift $f_{mn}(t)$ in the angular Doppler shift expression as $2\pi f_{mn}(t)t$, has been considered in many studies, e.g., [1], [11], [12], [18], [19]. However, this assumption is considered erroneous as it results in higher values of the local Doppler spread than physically expected [12]. Furthermore, it has been shown in [12] that the local Doppler spread derived from the local ACF and the time variant Doppler spread obtained from the PDF of the Doppler shift are equal only in the stationary case, i.e., if the speed acceleration and the angular speed of the MS are equal to zero. It is worthwhile to mention that the angular Doppler shift given by $2\pi f_{mn}(t)t$ has also been used in [1] which results in an inconsistent model in the sense that the time variant Doppler spread derived from the PDF $p_{f_{mn}}(f;t)$ is unequal to the local Doppler spread derived from the local ACF or, alternatively, from the corresponding Wigner-Ville spectrum. In this paper, by taking profit from the concept of instantaneous frequency, we could resolve this problem and develop an accurate and Doppler-spread-consistent channel model that incorporates the effect of velocity variations of the MSs.

E. PDF of the Envelope

Recall that the AOD α_m^T and the AOA α_n^R in (7) and (8), respectively, are i.i.d. random variables with uniform distribution over 0 to 2π. Therefore, the Doppler shifts $f_{mn}(t)$ reduce to random variables at any fixed point in time t. Consequently, for fixed values of t, the complex channel gain $\mu(t)$ in (27) can be analysed in the same way as conventional stationary fading processes. According to the central limit theorem [35, p. 278], the overall complex channel gain $\mu(t)$ in (27) can be described by the product of two zero-mean complex Gaussian processes $\mu_1(t)$ and $\mu_2(t)$ each with variance σ_0^2. Hence, the envelope $R(t) = |\mu(t)| = |\mu_1(t)|\,|\mu_2(t)|$ is given by the product of two independent Rayleigh processes. In this case, the gains

c_{mn} are supposed to be Rayleigh distributed with parameter $\sigma_c^2 = \sigma_0^2/(MN)$ [36]. The analytical expression for the PDF of the double Rayleigh process $R(t)$ is given by [37]

$$p_R(r) = \frac{r}{\sigma_0^4} K_0\left(\frac{r}{\sigma_0^2}\right) \tag{40}$$

where $K_0(\cdot)$ stands for the zeroth-order modified Bessel function of the second kind [30, Eq. (8.407-1)]. Note that the velocity variations of the transmitter T_x and the receiver R_x do not affect the distribution of the envelope process $R(t)$.

The above analysis of non-stationary channels has been conducted under the assumption of isotropic scattering. In reality, however, it has been shown in many experimental studies that this assumption is usually not fulfilled [38]–[40]. In addition, it has been demonstrated in [25] that non-stationarity in time contradicts the isotropic scattering assumption. Motivated by these facts, we extend the above analysis in the next section to non-isotropic scattering.

IV. Statistical Properties of the Reference Model Assuming Non-Isotropic Scattering

In this section, we specifically investigate the correlation properties of the non-stationary M2M channel model under non-isotropic scattering conditions. Towards this end, we employ the von Mises PDF [26] to describe the distributions of the AOD α_m^T and AOA α_n^R. In addition to its analytical tractability, the von Mises distribution is sufficiently versatile as it allows the approximation of the cardioid [41], the wrapped Gaussian [41], and the wrapped normal [42] distributions. The von Mises PDF is given by [26]

$$p_{\alpha_q^i}(\alpha_q^i) = \frac{\exp\left(\varkappa_i \cos\left(\alpha_q^i - \varphi_q^i\right)\right)}{2\pi I_0(\varkappa_i)} \tag{41}$$

where $I_0(\cdot)$ is the zeroth-order modified Bessel function of the first kind [30, Eq. (8.406.1)]. In (41), the letter $i \in \{T, R\}$ is used to refer to the transmitter (T) and the receiver (R), while the subscript $q \in \{m, n\}$ is associated with the mth scatterer around the transmitter and the nth scatterer around the receiver. The symbols φ_m^T and φ_n^R represent the mean values of the AOD α_m^T and the AOA α_n^R, respectively, whereas $\varkappa_T$ and $\varkappa_R$ control the angular spread of α_m^T and α_n^R, respectively. For the special case, if $\varkappa_i = 0$, the scattering is isotropic and the AOA α_n^R (AOD α_m^T) is uniformly distributed with $p_{\alpha_q^i}(\alpha_q^i) = 1/2\pi$. It is known from [38] that non-isotropic scattering has no influence on the first-order statistics of the complex channel gain $\mu(t)$, but it affects considerably the correlation properties of the channel and, thus, the corresponding Doppler power spectrum. Accordingly, we derive the local ACF of the proposed non-stationary M2M fading channel under non-isotropic scattering conditions. For convenience, the reference model described by the complex channel gain $\mu(t)$ in (27) is used here as a starting point. For the general case, where the transmitter T_x and the receiver R_x are moving with varying velocities, i.e., $a_0^i \neq 0$ and $b_0^i \neq 0$, where $i \in \{T, R\}$, the local ACF $r_{\mu\mu}(\tau, t)$ can be expressed by using [30, Eq. (3.937-2)] as in (42) [see the equation at the top of the next page]. By setting $\varkappa_T = \varkappa_R = 0$, it can be shown that (42) reduces to the ACF $r_{\mu\mu}(\tau, t)$ of the non-stationary M2M channel model under isotropic scattering conditions given in (31). We can notice that both the speed acceleration a_0^i and the angular speed b_0^i influence the local ACF $r_{\mu\mu}(\tau, t)$. Next, if the MSs are moving with variable speeds in a fixed direction, i.e., $\alpha_0^i \neq 0$ and $b_0^i = 0$, then the local ACF $r_{\mu\mu}(\tau, t)$ is obtained by taking the limit of (42) as $b_0^i \to 0$ which results in

$$\begin{aligned} r_{\mu\mu}(\tau, t) = {} & \frac{2\sigma_0^2}{I_0(\varkappa_T) I_0(\varkappa_R)} \\ & \cdot I_0\Bigg(\sqrt{\varkappa_T^2 - 4\pi^2\tau^2 f_{\max}^T(t) + 4\pi j f_{\max}^T(t)\varkappa_T \tau \cos\left(\varphi_m^T - \alpha_0^T\right)}\Bigg) \\ & \cdot I_0\Bigg(\sqrt{\varkappa_R^2 - 4\pi^2\tau^2 f_{\max}^R(t) + 4\pi j f_{\max}^R(t)\varkappa_R \tau \cos\left(\varphi_n^R - \alpha_0^R\right)}\Bigg). \end{aligned} \tag{43}$$

Furthermore, for the special case that a_0^i and α_0^i are set to zero, which corresponds to a stationary M2M channel model, (43) simplifies to the following known result of the ACF of the M2M model under non-isotropic scattering given in [20, Eq. (5)]

$$\begin{aligned} r_{\mu\mu}(\tau) = {} & \frac{2\sigma_0^2}{I_0(\varkappa_T) I_0(\varkappa_R)} \\ & \cdot I_0\Bigg(\sqrt{\varkappa_T^2 - 4\pi^2\tau^2 (f_{\max_0}^T)^2 + 4\pi j f_{\max_0}^T \varkappa_T \tau \cos\left(\varphi_m^T\right)}\Bigg) \\ & \cdot I_0\Bigg(\sqrt{\varkappa_R^2 - 4\pi^2\tau^2 (f_{\max_0}^R)^2 + 4\pi j f_{\max}^R \varkappa_R \tau \cos\left(\varphi_n^R\right)}\Bigg). \end{aligned} \tag{44}$$

If, in addition, $\varkappa_i$ is set to zero in (44), we obtain the ACF of the isotropic M2M channel model that has been presented in [33, Eq. (35)] in the form $r_{\mu\mu}(\tau) = 2\sigma_\mu^2 J_0\left(2\pi f_{\max_0}^T \tau\right) J_0\left(2\pi f_{\max_0}^R \tau\right)$.

Finally, we consider the scenario where only one MS is moving with variations in both speed and angle of motion. In this case, either the transmitter or the receiver is allowed to change its direction, i.e., $b_0^i \neq 0$ for either $i = T$ or $i = R$, whereas the direction of the other MS remains the same over the time, i.e., $b_0^l = 0$ for $l \neq i$. Thus, the local ACF $r_{\mu\mu}(\tau, t)$ is found to be given by the limit of (42) as $b_0^l \to 0$, which gives (45) [see the next page]. In (45), $q \in \{m, n\}$. The results above in (42), (43), and (45) show the impact of non-isotropic scattering on the local ACF $r_{\mu\mu}(\tau, t)$. For completeness, we mention that the Wigner-Ville spectrum $S_{\mu\mu}(f, t)$ of the non-stationary M2M fading channels, where the AOD and the AOA are non-uniformly distributed according to the von Mises distribution, can be obtained by inserting the local ACF $r_{\mu\mu}(\tau, t)$ given by (42) in (35).

V. Numerical Results

In this section, we present some numerical examples to illustrate the obtained analytical results for different propagation scenarios. In each scenario, the MSs follow different trajectories according to their velocity changes. For all trajectories, we have set the initial velocity v_0^i to 3 km/h and the initial angle of motion α_0^i to 0, where $i \in \{T, R\}$. The parameter σ_0^2 has been chosen equal to unity and the carrier frequency f_0

$$r_{\mu\mu}(\tau,t)=\frac{2\sigma_0^2}{I_0(\varkappa_T)I_0(\varkappa_R)}I_0\Bigg(\Bigg\{\varkappa_T^2-\left(\frac{4\pi}{b_0^T}f_{\max}^T(t)\right)^2\sin^2\left(b_0^T\frac{\tau}{2}\right)-\left(\frac{2\pi}{b_0^T}\dot{f}_{\max}^T\right)^2\left(\frac{2}{b_0^T}\sin\left(b_0^T\frac{\tau}{2}\right)-\tau\cos\left(b_0^T\frac{\tau}{2}\right)\right)^2$$
$$-8\pi j\frac{\varkappa_T}{b_0^T}\left(\frac{\dot{f}_{\max}^T}{b_0^T}\sin\left(\alpha_{\mathrm{v}}^T(t)-\varphi_m^T\right)\sin\left(b_0^T\frac{\tau}{2}\right)-f_{\max}^T(t)\cos\left(\alpha_{\mathrm{v}}^T(t)-\varphi_m^T\right)\sin\left(b_0^T\frac{\tau}{2}\right)-\dot{f}_{\max}^T\frac{\tau}{2}\sin\left(\alpha_{\mathrm{v}}^T(t)-\varphi_m^T\right)\cos\left(b_0^T\frac{\tau}{2}\right)\right)\Bigg\}^{\frac{1}{2}}\Bigg)$$
$$\cdot I_0\Bigg(\Bigg\{\varkappa_R^2-\left(\frac{4\pi}{b_0^R}f_{\max}^R(t)\right)^2\sin^2\left(b_0^R\frac{\tau}{2}\right)-\left(\frac{2\pi}{b_0^R}\dot{f}_{\max}^R\right)^2\left(\frac{2}{b_0^R}\sin\left(b_0^R\frac{\tau}{2}\right)-\tau\cos\left(b_0^R\frac{\tau}{2}\right)\right)^2$$
$$-8\pi j\frac{\varkappa_R}{b_0^R}\left(\frac{\dot{f}_{\max}^R}{b_0^R}\sin\left(\alpha_{\mathrm{v}}^R(t)-\varphi_n^R\right)\sin\left(b_0^R\frac{\tau}{2}\right)-f_{\max}^R(t)\cos\left(\alpha_{\mathrm{v}}^R(t)-\varphi_n^R\right)\sin\left(b_0^R\frac{\tau}{2}\right)-\dot{f}_{\max}^R\frac{\tau}{2}\sin\left(\alpha_{\mathrm{v}}^R(t)-\varphi_n^R\right)\cos\left(b_0^R\frac{\tau}{2}\right)\right)\Bigg\}^{\frac{1}{2}}\Bigg). \quad (42)$$

$$r_{\mu\mu}(\tau,t)=\frac{2\sigma_0^2}{I_0(\varkappa_i)I_0(\varkappa_l)}I_0\left(\left\{\varkappa_l^2-4\pi^2\tau^2f_{\max}^l(t)+4\pi jf_{\max}^l(t)\varkappa_l\tau\cos\left(\varphi_q^l-\alpha_0^l\right)\right\}^{\frac{1}{2}}\right)$$
$$\cdot I_0\Bigg(\Bigg\{\varkappa_i^2-\left(\frac{4\pi}{b_0^i}f_{\max}^i(t)\right)^2\sin^2\left(b_0^i\frac{\tau}{2}\right)-\left(\frac{2\pi}{b_0^i}\dot{f}_{\max}^i\right)^2\left(\frac{2}{b_0^i}\sin\left(b_0^i\frac{\tau}{2}\right)-\tau\cos\left(b_0^i\frac{\tau}{2}\right)\right)^2$$
$$-8\pi j\frac{\varkappa_l}{b_0^i}\left(\frac{\dot{f}_{\max}^i}{b_0^i}\sin\left(\alpha_{\mathrm{v}}^i(t)-\varphi_q^i\right)\sin\left(b_0^i\frac{\tau}{2}\right)+f_{\max}(t)\cos\left(\alpha_{\mathrm{v}}^i(t)-\varphi_q^i\right)\sin\left(b_0^i\frac{\tau}{2}\right)-\dot{f}_{\max}^i\frac{\tau}{2}\sin\left(\alpha_{\mathrm{v}}^i(t)-\varphi_q^i\right)\cos\left(b_0^i\frac{\tau}{2}\right)\right)\Bigg\}^{\frac{1}{2}}\Bigg). \quad (45)$$

has been set to 5.9 GHz. By changing the mobility parameters a_0^i and b_0^i, the total distance travelled by each mobile terminal varies over time. Here, we consider that the transmitter T_x and the receiver R_x are allowed to move along one of the three different trajectories illustrated in Fig. 2. In all trajectory scenarios, we have considered the same observation period [0, 5 s]. In the case of the first trajectory (Path I), the MS, i.e., either the transmitter T_x or the receiver R_x, is moving with variations in both speed and direction of motion. The speed acceleration is $a_0^i = 1.5$ m/s^2 and the angular speed is $b_0^i = \pi/10$ s^{-1}. However, for the second trajectory (Path II), the parameters $a_0^i = 0$ m/s^2 and $b_0^i = \pi/10$ s^{-1} have been selected. This implies that only the angle of motion $\alpha_{\mathrm{v}}^i(t)$ of the MS is changing over time while the speed $\mathrm{v}_i(t) = \mathrm{v}_0^i$ remains constant. The third trajectory (Path III) takes into account only the speed variations of the MS, i.e., $a_0^i = 1.5$ m/s^2 and $b_0^i = 0$. The numerical values of v_0^i and a_0^i have been adopted from [43] as realistic vehicle speeds in urban environments. Concerning the values of b_0^i, they have been chosen arbitrarily to generate three different trajectories for MSs. Therefore, in all cases, we can assume that the mobility range of the MS during the observation period [0, 5 s] is limited so that the proposed non-stationary channel model can be applied. It is noteworthy that the presented trajectories reflect the motion of vehicles in real-world urban environments, where the vehicles' velocities are influenced by many factors, including the traffic density, the road geometry, and the roadside environment. In what follows, we study three different propagation scenarios based on a combination of the presented trajectories. The key parameters of these scenarios are summarized in Table. I.

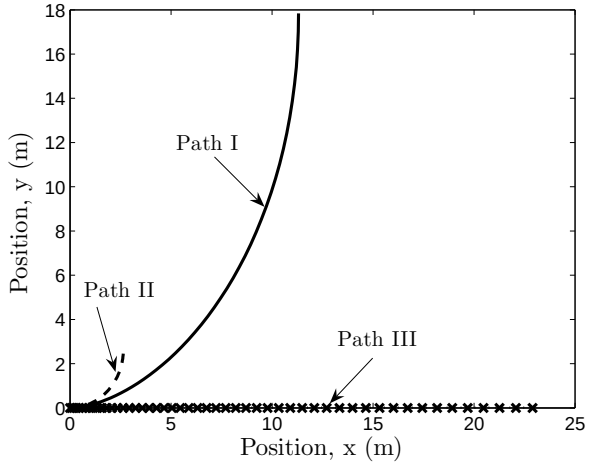

Fig. 2: Different trajectories along which the MSs can travel in the (x, y) plane.

A. Scenario I

In Scenario I, we suppose that the transmitter T_x is moving along Path I, whereas the mobile receiver R_x takes the route along Path II. Under these assumptions, the plot of the local ACF $r_{\mu\mu}(\tau, t)$ presented in (31) is shown in Fig. 3. Obviously, if the velocity of the transmitter MS increases with time t due to the acceleration, then the local ACF is decreasing over the time difference τ if t increases, meaning that the channel decorrelates faster with time. This finding is contradictory to the stationary case, where the correlation properties are independent of time and only a function of the time difference. This observation is also confirmed by Fig. 4 that depicts the

TABLE I: Parameters of the trajectories taken by T_x and R_x in different propagation scenarios.

Scenario	Speed Acceleration	Angular Speed	Maximum Speed (at t = 5 s)
I	$a_0^T = 1.5$ m/s^2 $a_0^R = 0$	$b_0^T = \frac{\pi}{10}$ s^{-1} $b_0^R = \frac{\pi}{10}$ s^{-1}	$v_T(t) = 30$ km/h $v_R(t) = 3$ km/h
II	$a_0^T = 1.5$ m/s^2 $a_0^R = 1.5$ m/s^2	$b_0^T = 0$ $b_0^R = 0$	$v_T(t) = 30$ km/h $v_R(t) = 30$ km/h
III	$a_0^T = 1.5$ m/s^2 $a_0^R = 1.5$ m/s^2	$b_0^T = \frac{\pi}{10}$ s^{-1} $b_0^R = \frac{\pi}{10}$ s^{-1}	$v_T(t) = 30$ km/h $v_R(t) = 30$ km/h

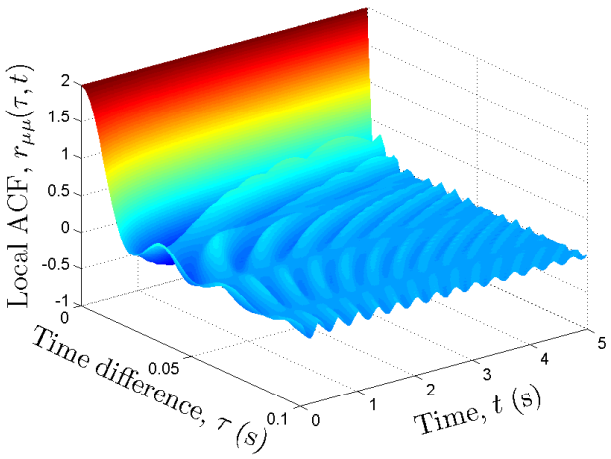

Fig. 3: Local ACF $r_{\mu\mu}(\tau, t)$ of the non-stationary M2M channel model for Scenario I.

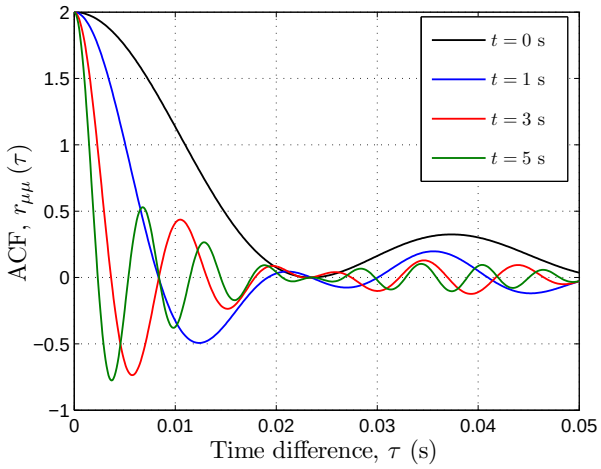

Fig. 4: ACF $r_{\mu\mu}(\tau)$ of the non-stationary M2M channel model for Scenario I for different time instants t.

behavior of the ACF $r_{\mu\mu}(\tau)$ of the proposed non-stationary M2M channel at different time instants t. By substituting (31) in (35), we obtain the Wigner-Ville spectrum $S_{\mu\mu}(f, t)$ which is plotted in Fig. 5. At the origin $t = 0$, we notice that the spectrum has the same shape as the spectrum of the corresponding stationary M2M fading channel model with a bandwidth given by $2\left(f^T_{\max_0} + f^R_{\max_0}\right)$ [33]. In Fig. 6, we plot the local Doppler spread $B^{(2)}_{\mu\mu}(t)$ [see (39)] derived from the local ACF $r_{\mu\mu}(\tau, t)$ and the time variant Doppler spread $B^{(2)}_{f_{mn}}(t)$ [see (17)] derived by means of the characteristic function $\psi_{f_{mn}}(\nu; t)$. As can be noticed from Fig. 6, the local Doppler spread $B^{(2)}_{\mu\mu}(t)$ coincides with the time variant Doppler spread $B^{(2)}_{f_{mn}}(t)$ which confirms the consistency of the proposed model with respect to the Doppler spread. The local Doppler spread $B^{(2)}_{\mu\mu}(t)$ is useful for studying the stationary interval (SI) which is defined as the maximum time interval during which the channel can be assumed to be WSS. For a given percentage change q, the SI T_q can be determined by the length of the time interval in which the maximum difference between $B^{(2)}_{f_{mn}}(T_q)$ and $B^{(2)}_{f_{mn}}(0)$ is q. For example, if $q = 20\%$, then it follows from Fig. 6 that the SI T_{20} is equal to 0.206 s.

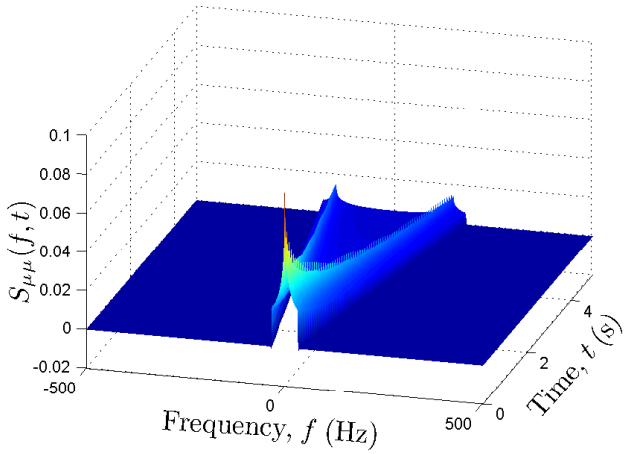

Fig. 5: Wigner-Ville spectrum $S_{\mu\mu}(f, t)$ of the non-stationary M2M channel model for Scenario I.

B. Scenario II

In Scenario II, both the transmitter T_x and the receiver R_x follow Path III. Thus, the MSs are moving with variations of the speed along a straight line. To account for the effects of the change of the speed over time, we plot the local ACF $r_{\mu\mu}(\tau, t)$ given by (33) in Fig. 7. Figure 8 also demonstrates the considerable difference between the ACFs $r_{\mu\mu}(\tau)$ taken at different points in time t due to the speed variation of the MSs. The plot of the corresponding Wigner-Ville spectrum is shown in Fig. 9. In this case, we notice that the Wigner-Ville spectrum

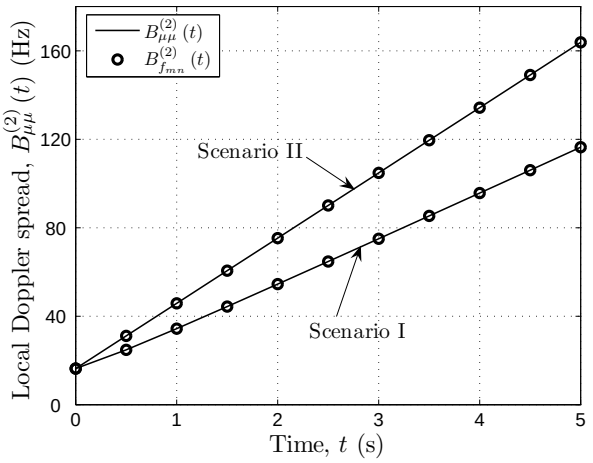

Fig. 6: Local Doppler spread $B^{(2)}_{\mu\mu}(t)$ for Scenarios I and II.

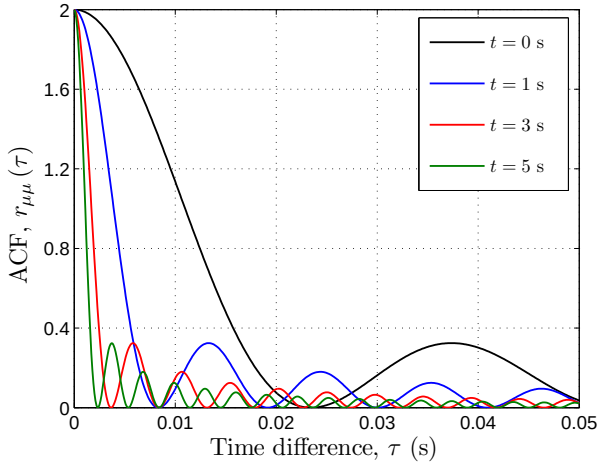

Fig. 8: ACF $r_{\mu\mu}(\tau)$ of the non-stationary M2M channel model for Scenario II for different time instants t.

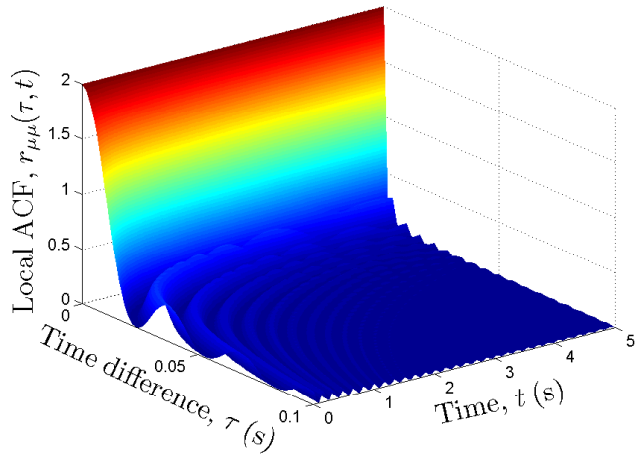

Fig. 7: Local ACF $r_{\mu\mu}(\tau, t)$ of the non-stationary M2M channel model for Scenario II.

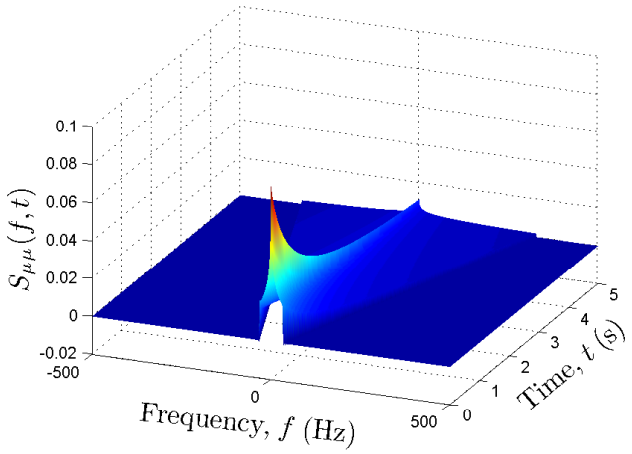

Fig. 9: Wigner-Ville spectrum $S_{\mu\mu}(f, t)$ of the non-stationary M2M channel model for Scenario II.

is proportional to the time variant PDF $p_{f_{mn}}(f; t)$ of the Doppler frequencies $f_{mn}(t)$ [see (12)]. Although the Wigner-Ville distribution satisfies many desirable properties, it is worth noting that the Wigner-Ville spectrum can have negative components, which represents a major drawback of this time-frequency representation. Thus, smoothing methods have been proposed to mitigate this problem [15]. In Scenario II, the resulting local Doppler spread $B^{(2)}_{\mu\mu}(t)$ is plotted and compared with the time variant Doppler spread $B^{(2)}_{f_{mn}}(t)$ in Fig. 6. Again, $B^{(2)}_{\mu\mu}(t)$ is shown to be equal to $B^{(2)}_{f_{mn}}(t)$ demonstrating that the physical inconsistency problem regarding the Doppler spread is solved by using the concept of the instantaneous frequency. In addition, we note that $B^{(2)}_{\mu\mu}(t)$ increases faster compared to the first scenario due to the increasing speed of the receiver ($a^R_0 = 1.5$ m/s^2). Therefore, The SI decreases in comparison with the SI of Scenario I, i.e., for the percentage change $q = 20\%$, the SI T_{20} is found to be equal to 0.11 s. This result shows that the SIs of NWSS channels are different according to the properties of the propagation scenarios.

C. Scenario III

In Scenario III, both the transmitter T_x and the receiver R_x take the route along the first trajectory. In this scenario, we assume non-isotropic scattering around T_x and R_x, where the AOD and the AOA are both assumed to follow the von Mises distribution. We have set the angular spreads to $\varkappa_T = \varkappa_R = 10$, while the mean values of the AOD and the AOA have been chosen to be equal to zero, i.e., $\varphi^T_m = \varphi^R_n = 0$. In this situation, we consider the expression of the local ACF $r_{\mu\mu}(\tau, t)$ given by (42), whose real part is plotted in Fig. 10, while the corresponding Wigner-Ville spectrum is illustrated in Fig. 11. It is worth mentioning that the imaginary part of the correlation function corresponds to the cross-correlation function of the inphase $\mu_I(t)$ and the quadrature $\mu_Q(t)$ components of $\mu(t) = \mu_I(t) + j\mu_Q(t)$. The cross-correlation function is equal (unequal) to zero under isotropic (non-isotropic) scattering conditions. From Fig. 10, we notice that at $t = 0$, the local ACF $r_{\mu\mu}(\tau, t)$ has the same form as the ACF $r_{\mu\mu}(\tau)$ of the stationary M2M model under non-isotropic scattering conditions [20].

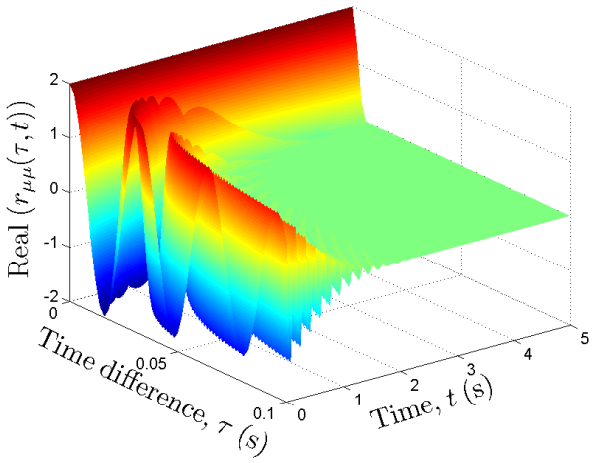

Fig. 10: Local ACF $r_{\mu\mu}(\tau,t)$ of the non-stationary M2M channel model for Scenario III.

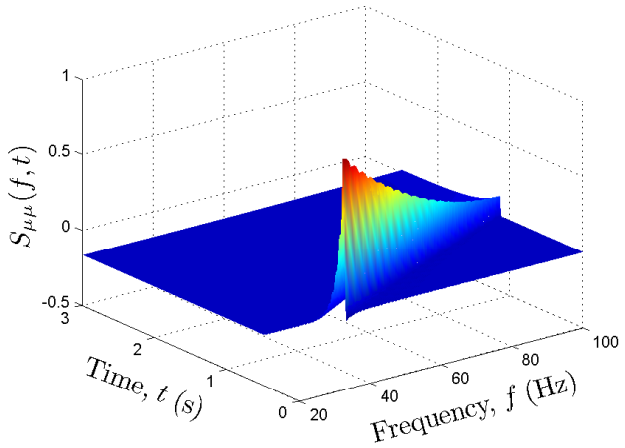

Fig. 11: Wigner-Ville spectrum $S_{\mu\mu}(f,t)$ of the non-stationary M2M channel model for Scenario III.

Nevertheless, the correlation decreases with time t if $\tau \neq 0$. Therefore, the Wigner-Ville spectrum $S_{\mu\mu}(f,t)$ is decreasing with time t as shown in Fig. 11. Moreover, it is observed that the local spectrum has an asymmetrical shape which is the consequence of the assumption of non-isotropic scattering.

VI. Conclusions

In this paper, we have presented a more realistic non-stationary SISO M2M fading channel model, wherein the transmitter and the receiver may experience changes of their velocities. Based on this model, we have analysed the impact of the variations of the speed and the direction of motion of the MSs on the statistical properties of the complex channel gain. By assuming an isotropic scattering scenario with double interactions between interfering objects and using time-frequency analysis techniques, we have presented analytical expressions for the local ACF, the Wigner-Ville spectrum, the local average Doppler shift, and the local Doppler spread. Although the results of the stationary case cannot be obtained directly from the derived expressions for the local ACF and the Wigner-Ville spectrum, the used time-frequency techniques have shown to be adequate for the analysis of non-stationary fading processes as they lead to consistent results with respect to the local average Doppler shift and the local Doppler spread. We have also investigated the correlation properties of the proposed model under non-isotropic scattering conditions. The obtained results include many well-known expressions derived under the assumption of isotropic scattering as special cases. The proposed reference model provides a theoretical framework for the development of a realizable simulation model. The development and the investigation of the statistical properties of the simulation model could be a topic for future work. Further extensions of this study could be made by incorporating the effects of moving scatterers and/or by considering a generalized three-dimensional scattering environment.

References

[1] W. Dahech, M. Pätzold, and N. Youssef, "A non-stationary mobile-to-mobile multipath fading channel model taking account of velocity variations of the mobile stations," in *9th European Conference on Antennas and Propagation (EuCAP'15)*, Lisbon, Portugal, Apr. 2015, pp. 1–4.

[2] A. Zajić, *Mobile-to-mobile wireless channels*, Artech House, 2012.

[3] A. F. Molisch, F. Tufvesson, J. Karedal, and C. F. Mecklenbräucker, "A survey on vehicle-to-vehicle propagation channels," *IEEE Wireless Commun. Mag.*, vol. 16, no. 5, pp. 12–22, Dec. 2009.

[4] B. Talha, S. Primak, and M. Pätzold, "On the statistical properties of equal gain combining over mobile-to-mobile fading channels in cooperative networks," in *Proc. International Conference on Communications (ICC'10)*, Cape Town, South Africa, May 2010.

[5] A. Goldsmith, *Wireless communications*, Cambridge University Press, 2005.

[6] M. Pätzold, *Mobile Radio Channels*, Chichester: John Wiley & Sons, 2nd edition, 2011.

[7] J. Karedal et al., "A geometry-based stochastic MIMO model for vehicle-to-vehicle communications," *IEEE Trans. Wireless Commun.*, vol. 8, no. 7, pp. 3646–3657, July 2009.

[8] M. Walter, D. Shutin, and U.-C. Fiebig, "Delay-dependent Doppler probability density functions for vehicle-to-vehicle scatter channels," *IEEE Transactions on Antennas and Propagation*, vol. 62, no. 4, pp. 2238–2249, Apr. 2014.

[9] S. Thoen, L. Van der Perre, and M. Engels, "Modelling the channel time-variance for fixed wireless communications," *IEEE Communications Letters*, vol. 6, no. 8, pp. 331–333, Aug. 2002.

[10] A. Borhani and M. Pätzold, "Correlation and spectral properties of vehicle-to-vehicle channels in the presence of moving scatterers," *IEEE Trans. Veh. Technol.*, vol. 62, no. 9, pp. 4228–4239, Nov. 2013.

[11] R. Iqbal and T. D. Abhayapala, "Impact of mobile acceleration on the statistics of Rayleigh fading channel," in *Proc. 8th Australian Communication Theory Workshop (AusCTW'07)*, Adelaide, Australia, Feb. 2007.

[12] M. Pätzold and A. Borhani, "A non-stationary multipath fading channel model incorporating the effect of velocity variations of the mobile station," in *Proc. Wireless Communication and Network Conference (WCNC'14)*, Istanbul, Turkey, Apr. 2014, pp. 194–199.

[13] L. Cohen, "Time-frequency distributions– A review," *Proceedings of the IEEE*, vol. 77, no. 7, July 1989.

[14] B. Boashash, *Time-Frequency Signal Analysis and Processing: A Comprehensive Reference*, Elsevier, 2nd edition, 2015.

[15] L. Cohen, *Time-Frequency Analysis*, Prentice Hall, 1995.

[16] M. Pätzold, B. O. Hogstad, and N. Youssef, "Modeling, analysis, and simulation of MIMO mobile-to-mobile fading channels," *IEEE Trans. Wireless Commun.*, vol. 7, no. 2, pp. 510–520, Feb. 2008.

[17] B. Boashash, "Estimating and interpreting the instantaneous frequency of a signal– Part 1: Fundamentals," *Proceedings of the IEEE*, vol. 80, no. 4, pp. 520–538, 1992.

[18] Y. Liu, Z. Tan, and X. Chen, "Modeling the channel time variation using high-order-motion mode," *IEEE Communications Letters*, vol. 15, no. 3, pp. 275–277, 2011.

[19] A. E. Abdelkareem, B. S. Sharif, C. C. Tsimenidis, and J. A. Neasham, "Time varying Doppler-shift compensation for OFDM-based shallow underwater acoustic communication systems," in *8th IEEE Int. Conf. on Mobile Adhoc and Sensor Systems (MASS'11)*, Oct. 2011, pp. 885–891.

[20] Y. R. Zheng, "A non-isotropic model for mobile-to-mobile fading channel simulations," in *IEEE Military Communication Conference (MILCOM'06)*, Washington, DC, USA, Oct. 2006, pp. 1–7.

[21] X . Cheng, C.-X. Wang, B . Ai, and H . Aggoune, "Envelope level crossing rate and average fade duration of nonisotropic vehicle-to-vehicle Ricean fading channels," *IEEE Trans. Intell. Transp. Syst.*, vol. 15, no. 1, pp. 62–72, 2014.

[22] W. Dahech, N. Hajri, N. Youssef, M. Pätzold, and T. Kawabata, "Level-crossing rate and average duration of fades in non-isotropic Hoyt fading channels with applications to selection combining diversity," in *Proc. IEEE 82nd Vehicular Technology Conference (VTC'15-Fall)*, Boston, USA, Sept. 2015, pp. 1–5.

[23] A. Chelli and M. Pätzold, "A non-stationary MIMO vehicle-to-vehicle channel model based on the geometrical T-junction model," in *Proc. International Conference on Wireless Communications and Signal Processing (WCSP'09)*, Nanjing, China, Nov. 2009.

[24] A. Borhani and M. Pätzold, "Modelling of non-stationary mobile radio channels incorporating the Brownian mobility model with drift," in *Proc. World Congress on Engineering and Computer Science (WCECS'13)*, San Francisco, USA, Oct. 2013, vol. II, pp. 695–700.

[25] A. Borhani and M. Pätzold, "A novel non-stationary channel model utilizing Brownian random paths," *REV Journal on Electronics and Communications (JEC)*, vol. 3, no. 1–2, pp. 8–15, 2014.

[26] A. Abdi, J. A. Barger, and M. Kaveh, "A parametric model for the distribution of the angle of arrival and the associated correlation function and power spectrum at the mobile station," *IEEE Trans. Veh. Technol.*, vol. 51, no. 3, pp. 425–434, May 2002.

[27] A. G. Zajić, G. L. Stüber, T. G. Pratt, and S. Nguyen, "Statistical modeling and experimental verification of wideband MIMO mobile-to-mobile channels in highway environments," in *Proc. 19th IEEE Int. Symp. on Personal, Indoor and Mobile Radio Communications (PIMRC'08)*, Cannes, France, Sept. 2008.

[28] A. G. Zajić, G. L. Stüber, T. G. Pratt, and S. Nguyen, "Statistical modeling and experimental verification of wideband MIMO mobile-to-mobile channels in urban environments," in *Proc. International Conference on Telecommunications (ICT'08)*, St. Petersburg, Russia, June 2008, pp. 1–6.

[29] R. H. Clarke, "A statistical theory of mobile-radio reception," *Bell Syst. Tech. Journal*, vol. 47, pp. 957–1000, July/Aug. 1968.

[30] I. S. Gradshteyn and I. M. Ryzhik, *Table of Integrals, Series, and Products*, Academic Press, 6th edition, 2000.

[31] R. J. Marks, *Handbook of Fourier analysis and its applications*, Oxford University Press, 2008.

[32] W. D. Mark, "Spectral analysis of the convolution and filtering of non-stationary stochastic processes," *Journal of Sound and Vibration*, vol. 11, no. 1, pp. 19–63, Jan. 1970.

[33] A. S. Akki and F. Haber, "A statistical model of mobile-to-mobile land communication channel," *IEEE Trans. Veh. Technol.*, vol. 35, no. 1, pp. 2–7, Feb. 1986.

[34] A. Bruscato and C. M. C. Toloi, "Spectral analysis of non-stationary processes using the Fourier transform," *Brazilian Journal of Probability and Statistics*, vol. 18, pp. 69–102, 2004.

[35] A. Papoulis and U. S. Pillai, *Probability, Random Variables and Stochastic Processess*, Mc Graw Hill, 4 edition, 2002.

[36] M. Pätzold and G. Rafiq, "Sparse multipath channels: modelling analysis, and simulation," in *Proc. 24th IEEE Int. Symp. on Personal, Indoor and Mobile Radio Communications, PIMRC 2013*. Sept. 2013, pp. 30–35, London, UK.

[37] I. Z. Kovács, *Radio channel characterization for private mobile radio systems: Mobile-to-mobile radio link investigations*, Ph.D. thesis, Aalborg University, Denmark, Feb. 2003.

[38] W. C. Y. Lee, "Finding the approximate angular probability density function of wave arrival by using a directional antenna," *IEEE Transactions on Antennas and Propagation*, vol. 21, no. 3, pp. 328–334, 1973.

[39] P. C. Fannin and A. Molina, "Analysis of mobile radio channel sounding measurements in inner city Dublin at 1.808 GHz," *IEE Proc. Commun.*, vol. 143, no. 5, pp. 311–316, 1996.

[40] J. Fuhl, J.-P. Rossi, and E. Bonek, "High-resolution 3-D direction-of-arrival determination for urban mobile radio," *IEEE Transactions on Antennas and Propagation*, vol. 45, no. 4, pp. 672–682, 1997.

[41] K. V. Mardia, *Statistics of directional data*, London: Academic, 1972.

[42] D . Collett and T. Lewis, "Discriminating between the von Mises and

wrapped normal distributions," *Australian Journal of Statistics*, vol. 23, no. 1, pp. 73–79, 1981.

[43] G. M. Morrison and S. Rauch, *Highway and Urban Environment: Proceedings of the 8th Highway and Urban Environment*, vol. 12, Springer Science & Business Media, 2007.

Wiem Dahech received the B.E. degree in computer networks and telecommunications from the "Institut National des Sciences Appliquées et de la Techologie", Tunisia, in 2011 and the M.S. degree in electronic systems and communication networks from the "Ecole Polytechnique de Tunisie", in 2012. She is currently a Ph.D. student in the "Ecole Supérieure des Communications de Tunis", Tunisia.

Matthias Pätzold (M'94−SM'98) received the Dipl.-Ing. and Dr.-Ing. degrees in electrical engineering from Ruhr-University Bochum, Bochum, Germany, in 1985 and 1989, respectively, and the habil. degree in communications engineering from the Technical University of Hamburg, Harburg, Germany, in 1998. From 1990 to 1992, he was with ANT Nachrichtentechnik GmbH, Backnang, Germany, where he was engaged in digital satellite communications. From 1992 to 2001, he was with the Department of Digital Networks, Technical University of Hamburg. Since 2001, he has been a Full Professor of mobile communications with the University of Agder, Grimstad, Norway. He is the author of several books and numerous technical papers. His publications received thirteen best paper awards. He has been actively participating in numerous conferences, serving as a member and as a Chair of technical program committees. He is currently an Associate Editor of the IEEE Vehicular Technology Magazine.

Carlos A. Gutiérrez received the B.E. degree in electronics and digital communication systems from the Autonomous University of Aguascalientes, Mexico, in 2002, the Advanced Studies Diploma (DEA) in signal processing and communication theory from the Polytechnic University of Catalonia (UPC), Spain, in 2005, the M.S. degree in electronics and telecommunications from CICESE, Mexico, in 2006, and the Ph.D. degree in mobile communication systems from the University of Agder, Norway, in 2009. From 2009 to 2011 he was with the School of Engineering, Universidad Panamericana Campus Aguascalientes, Mexico. Since January 2012, he is with the Faculty of Science, Universidad Autonoma de San Luis Potosí, Mexico. His research interests include modeling and simulation of mobile fading channels for wireless communication systems, and physical layer aspects of OFDM and MC-CDMA systems. He has served as guest editor for the journals Modelling and Simulation in Engineering, Procedia Technology, and Research in Computing Science, and as TPC member for various international conferences. Dr. Gutierrez is a member of the Mexican National System of Researchers (SNI).

Néji Youssef received the B.E. degree in telecommunications from the "Ecole des Postes et des Télécommunications de Tunis", Tunisia, in 1983, and the D.E.A. in electrical engineering from the "Ecole Nationale d'Ingénieurs de Tunis", in 1986. He also received the M.E. and Ph.D. degrees in communication engineering from the University of Electro-Communications, Tokyo, Japan, in 1991 and 1994, respectively. From 1994 to 1996, he was a Research Associate at the University of Electro-Communications, Tokyo. Since 1997, he joined the "Ecole Supérieure des Communications de Tunis", where he is currently a Professor. His research interests include noise theory, modeling of multipath fading channels and performance analysis of wireless communications.

January 24, 2017